Volume 15, Number 4, 2022. pp. 331-341

Jordan Journal of Physics

ARTICLE

Shielding Properties of Glass Samples Containing Li_2O, K_2O, Na_2O, PbO and B_2O_3 by Geant4, XCOM and Experimental Data

Ali H. Taqi, Abdulahdi M. Ghalib and **Shlair I. Mohammed**

Department of Physics, College of Science, Kirkuk University, Kirkuk, Iraq.

Doi: **https://doi.org/10.47011/15.4.1**

Received on: 21/09/2020; *Accepted on: 05/04/2021*

Abstract: In the present work, glass samples containing $10Li_2O$, $10K_2O$, $20Na_2O$. xPbO, $(60\text{-}x)B_2O_3$ (where x = 0-60) were prepared by the melt quenching method. The shielding parameters of the prepared samples were measured experimentally and calculated theoretically. The measurements have been performed at energies of 356.5, 662, 1173 and 1333 keV to obtain the total mass attenuation coefficient (μ_m), using a gamma spectrometer containing a shielded NaI (TI) detector. The results of mass attenuation coefficient (μ_m), half-value layers (HVLs), mean free path (MFP), radiation protection efficiency (RPE), atomic and electronic electron cross-sections (σ_a and σ_e), effective atomic number (Z_{eff}) and effective electron number (N_{eff}) were calculated at energies from 1 keV to 100 GeV using the Monte Carlo simulation code Geant4 and XCOM. The calculated results were compared with each other and with the experimental values. Good agreement has been observed.

Keywords: Shielding properties, Glass, Photon mass attenuation coefficient, Atomic and electronic cross-sections, Effective atomic and electron numbers, XCOM, Geant4.

Introduction

Exposure to or using ionizing rays can cause damage. Such damage can be controlled, particularly by the shielding method, because it gives a good working-safety level [1]. The study of interaction of radiation with matter is an important research field for the evolution of substances that can be used in a high-radiation setting [2-4]. The intensity of the radiation gradually decreases, as a result of a sequence of interactions, where the linear attenuation coefficient (μ) can be defined as the probability per unit length that a radiation will undergo an interaction in the material [5]. Due to the many and important uses of radioactive isotopes in medical and industrial applications, it became necessary to evolve materials that are used in protection [6].

There is an ongoing need to find more designs suitable for radiation protection. The shielding parameters, such as total linear attenuation coefficient (μ), mass attenuation coefficient ($\mu_m=\mu/\rho$), half-value layers (HVLs), mean free path (MFP), radiation protection efficiency (RPE), electronic and atomic cross sections (σ_e and σ_a), effective atomic and electron numbers (Z_{eff} and N_{eff}), are major for testing materials in radiation protection [7]. From the shielding point of view, it is known that an increase in μ_m, Z_{eff} and N_{eff} values enhances the gamma-ray shielding properties, while less MFP and HVL values clearly indicate improving the gamma-ray shielding performance of the absorbent material.

Glass has a set of features that make it useful and important in radiation shielding, like transparency, high homogeneity that can be attained and accepting a wide range of composition. Many experimental and theoretical

Corresponding Author: Ali H. Taqi **Email**: alitaqi@uokirkuk.edu.iq

studies of glass shielding parameters have been investigated at different energies, such as bismuth borate glasses [8], $PbO–SiO_2$ glasses [9], xPbO:(100-x) B_2O_3 glasses at 662 keV [10], phosphate glass containing Bi_2O_3, PbO and BaO at 662 keV [11], silicate glasses containing Bi_2O_3, BaO and PbO in the energy region of 1 keV to 100 GeV [12], lead zinc borate glasses [13], heavy-metal oxide glasses [14, 15], PbO-Li_2O-B_2O_3 glasses [16], PbO-B_2O_3, PbO-SiO_2, PbO-GeO_2 and PbO-WO_3-TeO_2 glass systems [17], xPbO-(100-x) P_2O_5 glasses [18] and PbO-Na_2O-B_2O_3-CaO-Al_2O_3-SiO_2 glasses [19].

The purpose of this study is to prepare glass samples containing $10Li_2O$. $10K_2O$. $20Na_2O$. xPbO. (60-x)B_2O_3, where x varies between 0 and 60. We studied the shielding parameters of the samples theoretically by using the Monte Carlo simulation code Geant4 and the XCOM program in the energy range of 1 keV-100 GeV. This was experimentally investigated by using a gamma spectrometer that contains a shielded NaI(Tl) detector at the energies of (356.5 keV)^{133}Ba, (662 keV)^{137}Cs, (1173, 1333 keV)^{60}Co. The calculated results will be compared between XCOM and Geant4 and compared with the experimental values.

Theory

The total mass attenuation coefficient ($\mu_m=\mu/\rho$) measures the gamma photon interaction probability (absorption or scattering) with the matter. The μ_m can be used to evaluate different shielding parameters. The common methods to evaluate μ_m of any material is explained with the following Lambert-Beer law [20, 21]:

$$I = I_0 e^{-\mu_m x \rho} \tag{1}$$

where I and I_0 are photon intensity with sample and without sample, ρ (g cm^{-3}) and x(cm) are the material density and the absorber thickness, respectively. μ_m of chemical compounds in terms of the weight fraction w_i can be calculated by [22]:

$$\mu_m = \sum_i w_i \, (\mu_m)_i \tag{2}$$

where w_i is expressed in terms of the atomic weight A as:

$$w_i = \frac{n_i A_i}{\sum_j n_j A_j} \tag{3}$$

where n_i is the number of formula units.

The half-value layer (HVL) is important to determine the material effectiveness against radiation and can be obtained by:

$$\mathrm{HVL} = \frac{\ln(2)}{\mu}\,. \tag{4}$$

Reducing the photon intensity by 1/e is known as the mean free path (MFP):

$$\mathrm{MFP} = \frac{1}{\mu}\,. \tag{5}$$

The effective atomic number (Z_{eff}) can be expressed in terms of the total atomic effective cross-section (σ_a) and the total electronic effective cross-section (σ_e) [23]:

$$Z_{\mathrm{eff}} = \frac{\sigma_a}{\sigma_e} \tag{6}$$

where σ_a and σ_e are evaluated by the following equations:

$$\sigma_a = \frac{1}{N_A}\sum_i f_i A_i \,(\mu_m)_i \tag{7}$$

$$\sigma_e = \frac{1}{N_A}\sum_i \frac{f_i A_i}{Z_i} (\mu_m)_i. \tag{8}$$

Z_{eff} is closely related to the average number of electrons per unit mass N_e [22]:

$$N_e = \frac{\mu_m}{\sigma_e} \tag{9}$$

The radiation protection efficiency (RPE) value can be obtained using the following expression:

$$\mathrm{RPE} = (1 - I/I_0) \times 100\,. \tag{10}$$

Materials and Methods

Sample Preparation

In the present work, seven glass samples were prepared using the melt quenching technique for the chemical formula: $10Li_2O$. $10K_2O$. $20Na_2O$. xPbO. (60-x) B_2O_3, where x takes the values 0, 10, 20, 30, 40, 50 and 60. Pure powder of the chemical compounds: H_3BO_3, Li_2CO_3, K_2CO_3, Na_2CO_3, PbO were used in the preparation of the samples. These compounds were weighed using an electronic balance having an accuracy of the order of 0.001g and mixed in a mortar for 10 minutes to prepare a 20-g batch of each composition. The alumina ceramic crucible containing the mixture was placed in an electric furnace at 1000 °C for 1 hour until being fully molten. The molten mixture will be converted into oxides of Li_2O, K_2O, Na_2O, PbO, and B_2O_3. The molten mixture was poured into a stainless steel mold inside an annealing furnace at 200 °C and kept for 2 hours, then slowly cooled to room temperature. The density of the investigated glass samples was measured using the Archimedes principle. The symbols and the densities of the prepared glass samples are given in Table 1, where the concentration of PbO and B_2O_3 varies from 0 to 60%, respectively.

Experimental Procedures

The experimental measurements were performed using a gamma spectrometer containing an NaI(TI) detector. The experimental arrangement is shown in Fig. 1. To reduce the background radiation, the whole system was shielded with 5 cm lead, 0.5 cm copper and 0.5 cm steel. The radioactive sources ^{133}Ba (356.5 keV), ^{137}Cs (662 keV), ^{60}Co (1173, 1333 keV) were used to obtain the mass attenuation coefficients. The background of the system is taken for 900s, the number of counts I_o of gamma particles was measured for each path length and then, by inserting the glass sample, the number of gamma counts I was recorded.

The theoretical calculations of the investigated samples are carried out by XCOM program and simulated by the Monte Carlo code Geant4 at the photon energies 1 keV-100 GeV. The gamma-ray shielding parameters of the prepared glass samples as functions of the incident photon energy and the chemical composition were calculated.

TABLE 1. Symbols and densities of the prepared glass samples.

Symbol	Composition $10Li_2O.10K_2O.20Na_2O.xPbO.(60\text{-}x)B_2O_3$ x varied as 0, 10, 20, 30, 40, 50 and 60	ρ(g cm^{-3})
S1	$10Li_2O.10K_2O.20Na_2O.0PbO.60B_2O_3$	2.3724
S2	$10Li_2O.10K_2O.20Na_2O.10PbO.50B_2O_3$	3.0699
S3	$10Li_2O.10\ K_2O.20Na_2O.20PbO.40B_2O_3$	3.3904
S4	$10\ Li_2O.10K_2O.20Na_2O.30PbO.30B_2O_3$	3.8453
S5	$10Li_2O.10K_2O.20Na_2O.40PbO.20B_2O_3$	4.0063
S6	$10Li_2O.10K_2O.20Na_2O.50PbO.10B_2O_3$	4.4495
S7	$10Li_2O.10K_2O.20Na_2O.60PbO.0B_2O_3$	5.0863

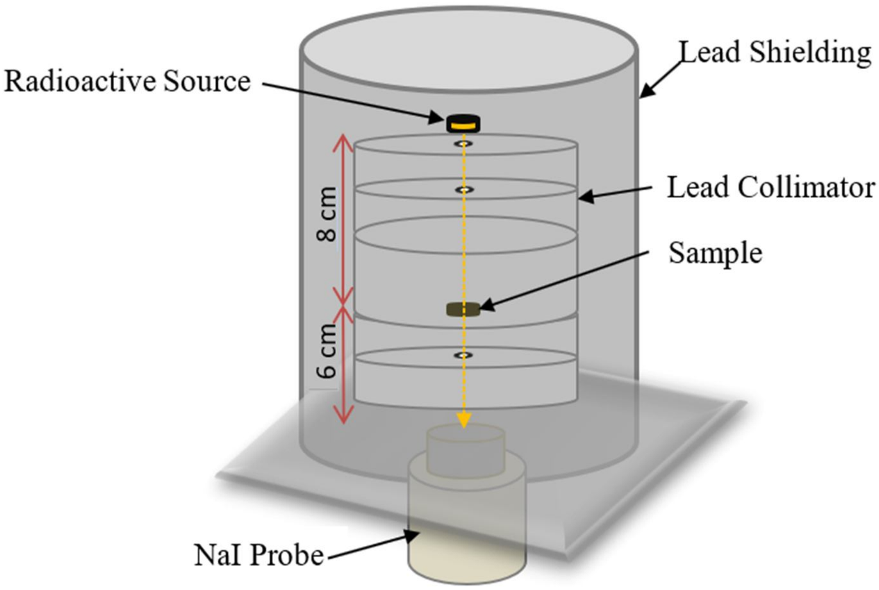

FIG. 1. Experimental arrangement to obtain the gamma attenuation coefficients.

Computational Methods

The computational calculations of the prepared glass samples were carried out using XCOM program and simulated by the Monte Carlo code Geant4 within the photon energy range from 1 keV to 100 GeV; then, all the parameters of radiation shielding were calculated as functions of the energy of the incident photon.

All the elements, materials and compounds were defined. The geometry is constructed to evaluate the initial and final numbers of photons before and after passing the samples (I_0 and I of Eq. 1), respectively. The XCOM program is available online, while the Gent4 code for windows has been installed and the TestEM13 project was executed after setting the type of the particle and its energy. More details can be found in Ref. [24].

Results and Discussion

The theoretical μ_m values of the prepared glass samples have been evaluated at the photon energies ranging from 1 keV to 100 GeV using the XCOM program and the simulation code Geant4. To understand the change of the μ_m values with photon energy, the obtained results are plotted in Fig. 2 and compared to the experimental values. It is seen that μ_m decreases when the photon energy increases to 15 MeV and many peaks are observed in the low photon energy region (< 100 keV) due to the K–, L– and M–photoelectric absorption edges. The sudden increases in μ_m are due to photoelectric absorption of photons, which usually occurs at an energy just above the binding energy of the electron in the shell.

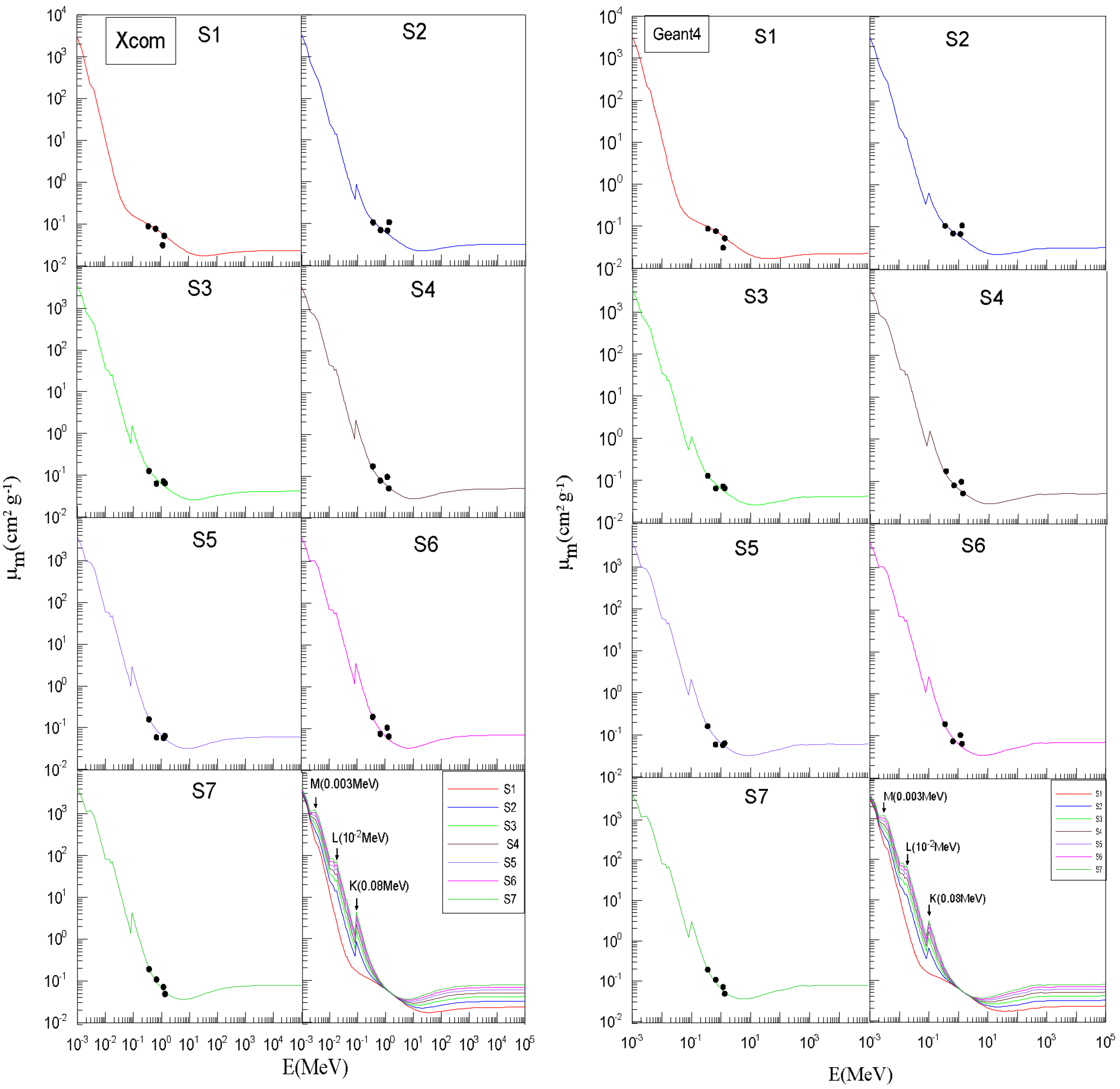

FIG. 2. Calculated μ_m values of the prepared glass samples in comparison with our experimental data.

As can be seen from Fig. 2, the behavior of μ_m against photon energy depends on the chemical composition of the prepared samples and on the nature of the photon interaction with the samples, which includes three main processes: photoelectric effect, Compton scattering and pair-production, where the effects of the three processes vary according to energies.

The values of μm, taken by using XCOM program, were slightly higher than Geant4 code values for low energies. The relative deviations between the calculated results of Geant4 and XCOM, defined as:

$$RD\% = ((\mu_m)_{XCOM} - (\mu_m)_{Geant4}/ (\mu_m)_{XCOM}) \times 100),$$

are plotted in Fig. 3. There is a satisfactory agreement between experiment and theory. The experimental data was lower than the theoretical values; therefore, the Geant4 values are more close to the experiment.

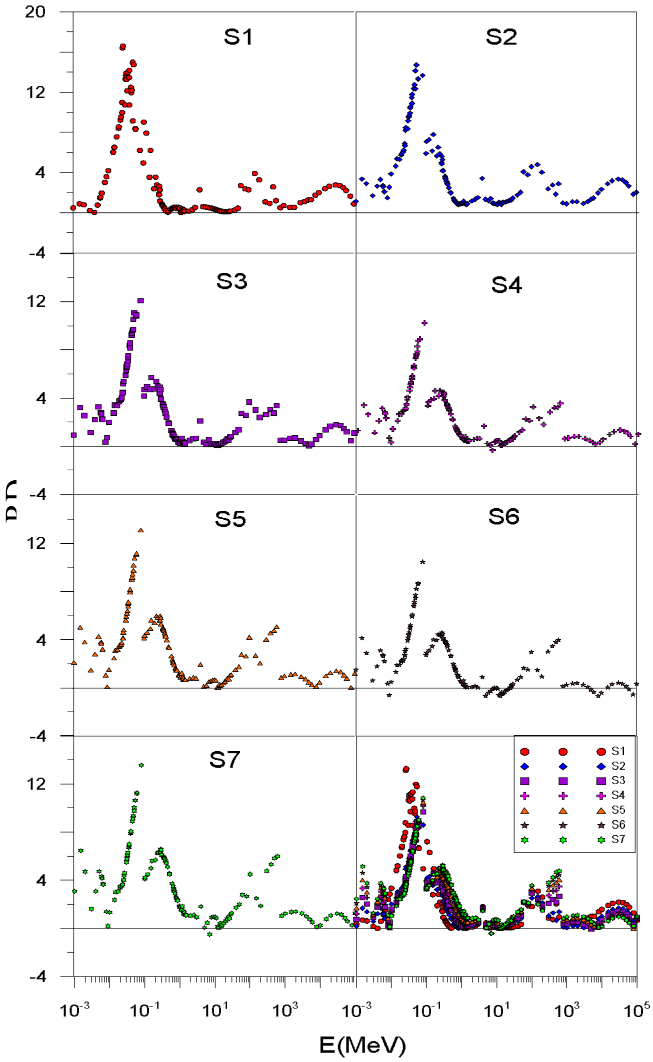

FIG. 3. Relative difference (RD%) between XCOM and Geant4 results of the investigated glass samples at the energy range (1 keV-100 GeV).

The radiation shielding features are observed to be significantly enhanced, by adding heavy elements to the prepared glass samples, as shown in Fig. 4. Although the increase in PbO concentration causes an increase in μ_m, yet the B_2O_3 concentration will decrease which will affect the transparency of the glass samples. The absorption edge increased with increasing the PbO concentration. Our results are compatible with the results of Refs. [16, 25], as illustrated in Table 2.

The variations of the half-value layers (HVLs) and the mean free path (MFP) of the investigated glass samples are illustrated in Figs. 5 and 6, respectively at photon energies varying from 1 keV to 100 GeV. It has been found that the HVL and MFP values are initially low and increase gradually with an increase in the incident photon energy up to 3 MeV. Above 3 MeV, the rate of decrease of HVL and MFP values is weak with the incident energy. It is clear that the increase in the PbO concentration leads to a decrease in the HVL and MFP values. Also, it was found that the absorption edges of sample S7 are lower than the absorption edges of the other samples, as shown in Figs. 5 and 6. The radiation protection efficiencies (RPEs) of the prepared glasses are presented in Table 3, where sample S7 is observed to possess high values of RPE.

TABLE 2. Experimental values of μ_m of the investigated glass samples in comparison with those of Refs. [16, 25].

E (keV)	$10Li_2O.10K_2O.20Na_2O.0PbO.60B_2O_3$ Sample S1 of this work	$35PbO.25Li_2O.40B_2O_3$ Ref. [16]	$35Li_2O.10ZnO.55B_2O_3$+ $0MnO_2$wt% Ref. [25]
	μ_m (cm^2 g^{-1})	μ_m (cm^2 g^{-1})	μ_m (cm^2 g^{-1})
356.5	0.0875	0.2150	0.0962
662	0.0762	0.0968	0.0742
1173	0.0679	0.0589	0.0566
1333	0.0515	0.0539	0.0532
	$10Li_2O.10K_2O.20Na_2O.60PbO.0B_2O_3$ Sample S7 of this work	$60PbO.0Li_2O.40B_2O_3$ Ref. [16]	$35Li_2O.10ZnO.55B_2O_3$+ $2MnO_2$wt% Ref. [25]
356.5	0.1916	0.2400	0.0965
662	0.1082	0.1010	0.0744
1173	0.0713	0.0601	0.0568
1333	0.0646	0.0551	0.0534

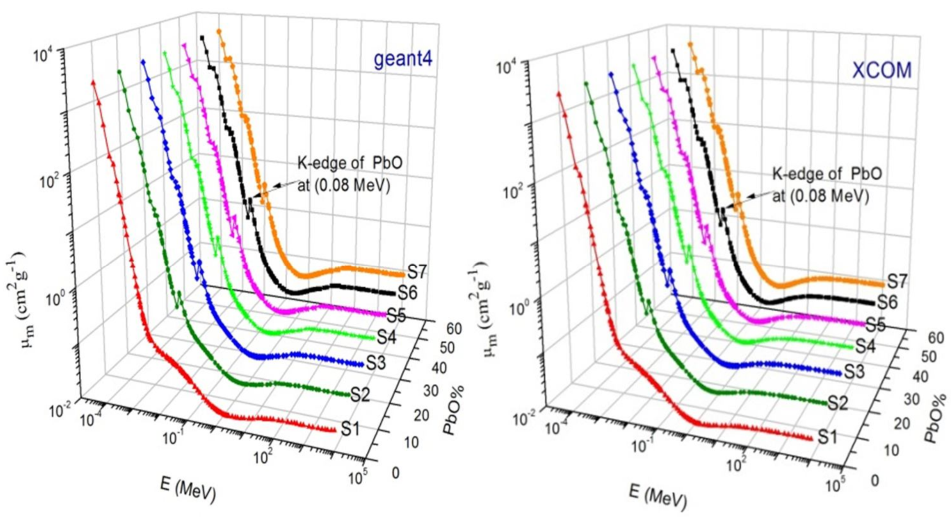

FIG. 4. XCOM and Geant4 mass attenuation coefficient values compared with PbO concentrations of the prepared samples.

TABLE 3. Radiation protection efficiency RPE of the investigated glass samples S1, S5 and S7.

E (keV)	RPE (%) S1	S5	S7
356.5	13.13097	40.18667	54.51057
662	11.53693	17.26499	35.89933
1173	4.83808	16.67967	25.92019
1333	7.961957	18.50337	18.07065

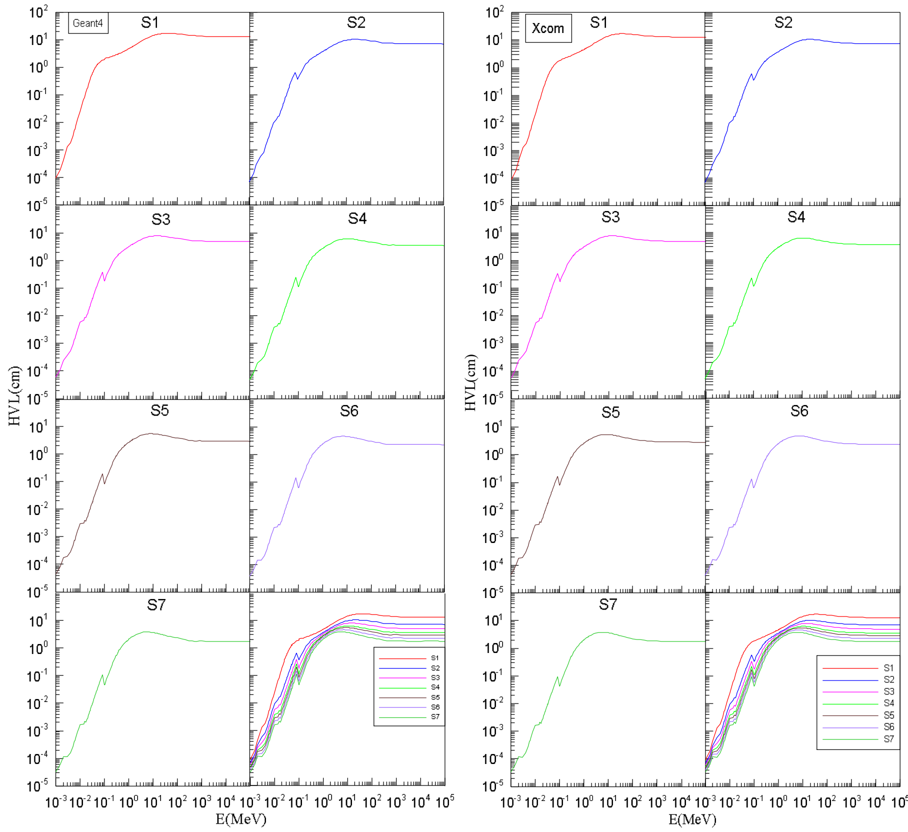

FIG. 5. Calculated half-value layers (HVLs) for the prepared samples against energy ranging from 1 keV to 100 GeV using the XCOM program and the simulation code Geant4.

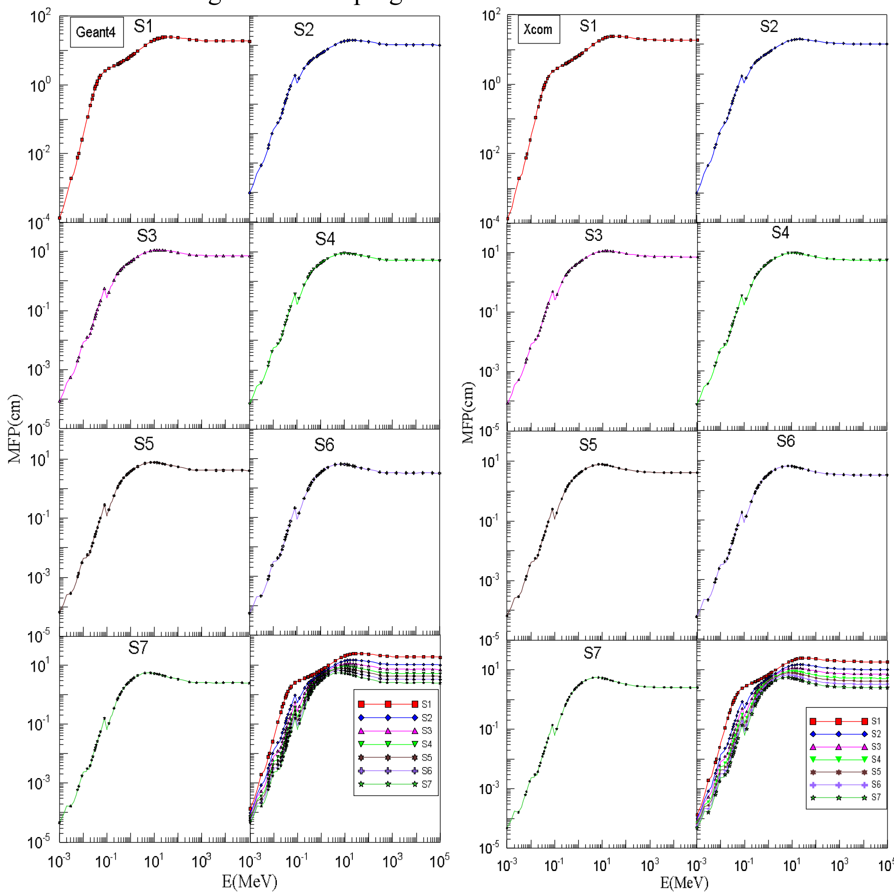

FIG. 6. Calculated mean free path (MFP) for the prepared samples against energy ranging from 1 keV to 100 GeV using the XCOM program and the simulation code Geant4.

The Geant4 and XCOM calculations of the atomic and electronic cross-sections (σ_a and σ_e) in the photon energy range (1 keV-100 GeV) are presented in Figs. 7 and 8. The results show that the cross-sections decrease with the energy of the incident photon for all the investigated samples and the cross-sections improved by increasing the PbO concentration over the energy range, due to high *A*. The photoelectric and pair production effects are dominant by high *A* of samples at low- and high-energy regions. The Compton effect predominates gradually and is almost independent of *A* of the constituent elements at the intermediate-energy region.

The Geant4 and XCOM calculations of the effective atomic number (Z_{eff}) and the effective electron number (N_{eff}) for the prepared glass samples in the photon energy range (1 keV-100 GeV) are illustrated in Figs. 9 and 10. Z_{eff} and N_{eff} values of the prepared samples increase with the increase of PbO concentration. The Z_{eff} and N_{eff} values show a broad peak and a maximum value at 0.01 MeV and a minimum at 1 MeV. Above 1 MeV, the values tend to be constant. The discontinuous jumps in Z_{eff} and N_{eff} for the low-energy region (< 100 keV) may be related to the photoelectric absorption edge of Pb, which is shown in Fig. 2, where the sharp peak is observed at 0.08 MeV due to K absorption edge. Also, the variations of Z_{eff} and N_{eff} with photon energy may be attributed to the relative domination of the photoelectric effect, Compton scattering and pair production, at different energy regions. The minimum Z_{eff} is found in the intermediate-energy region (around 1 MeV). In this region, Compton scattering is the dominant photon interaction process. Beyond 1 MeV, the Z_{eff} value increases because of the fact that the predominance of pair production ends to be constant. Our findings are consistent with those of Ref. [17].

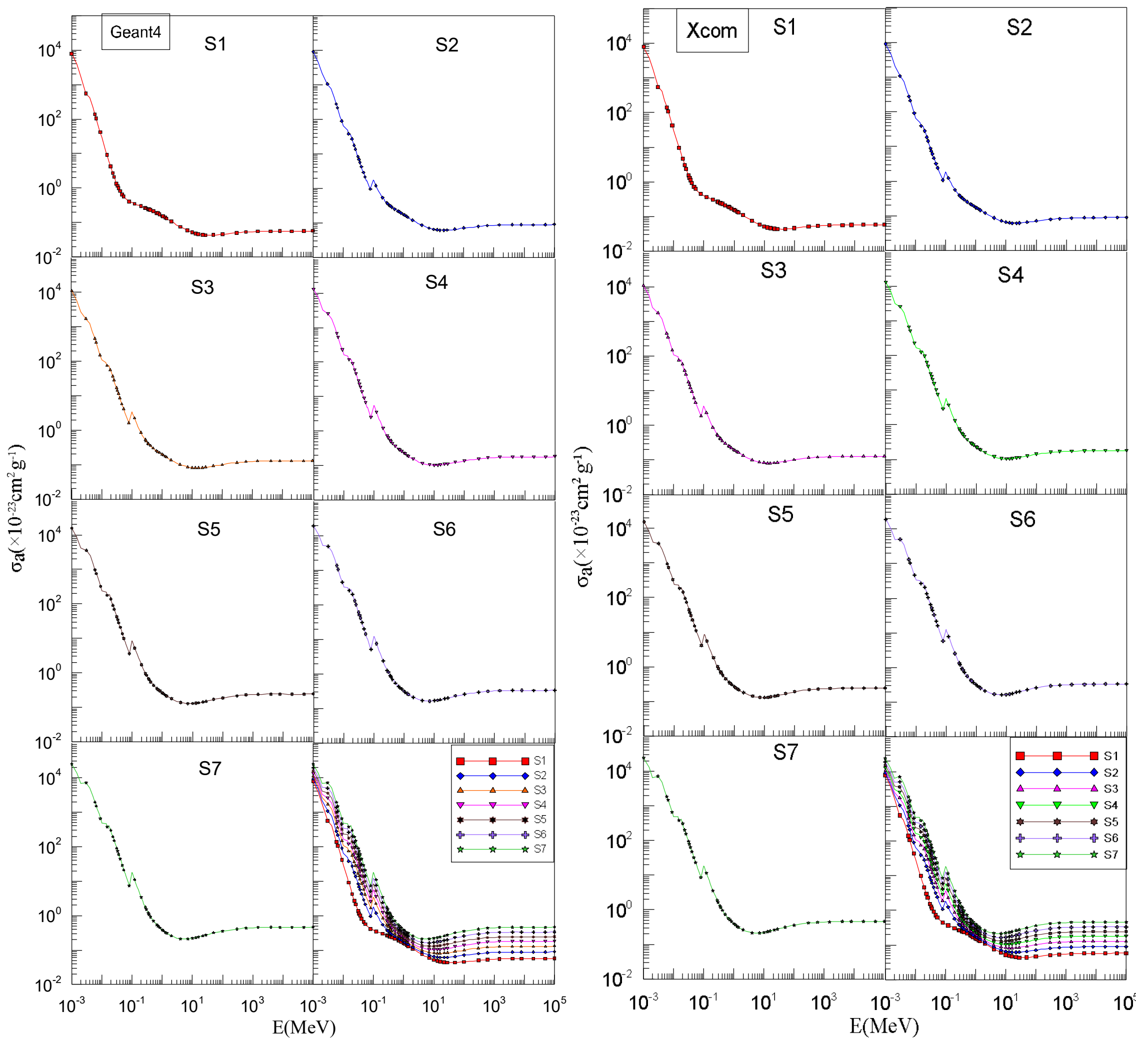

FIG. 7. Calculated atomic cross-sections (σ_a) for the prepared samples against energy ranging from 1 keV to 100 GeV using the XCOM program and the simulation code Geant4.

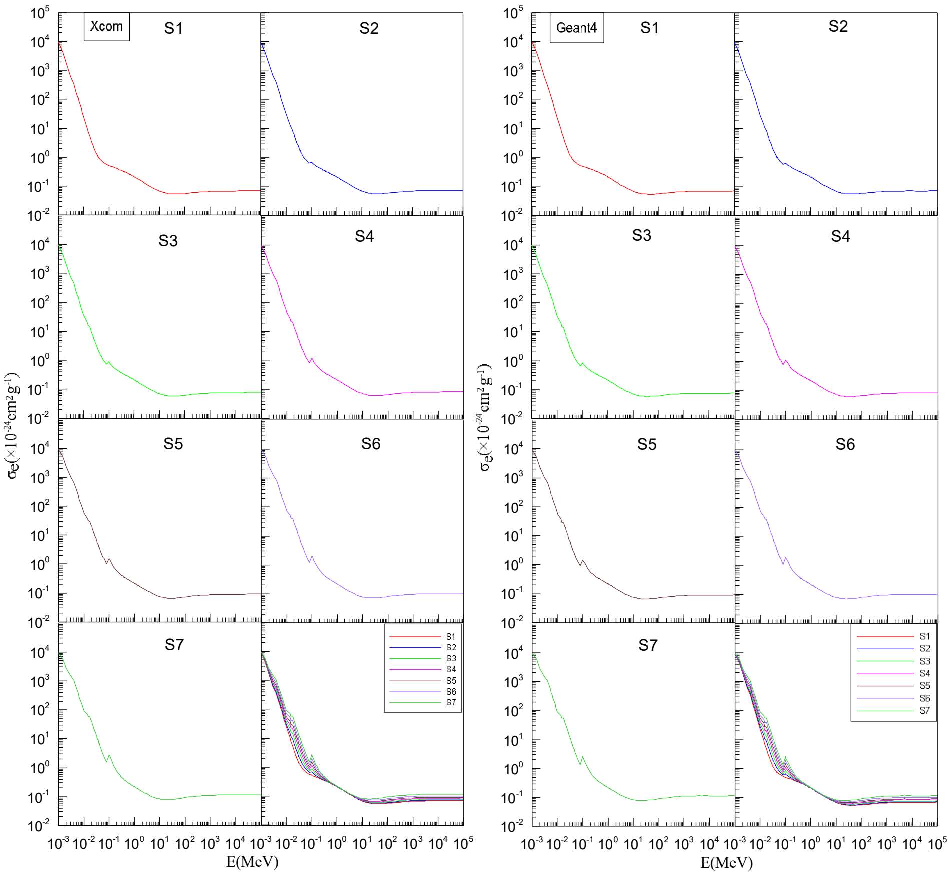

FIG. 8. Calculated electron cross-sections (σ_e) for the prepared samples against energy ranging from 1 keV to 100 GeV using the XCOM program and the simulation code Geant4.

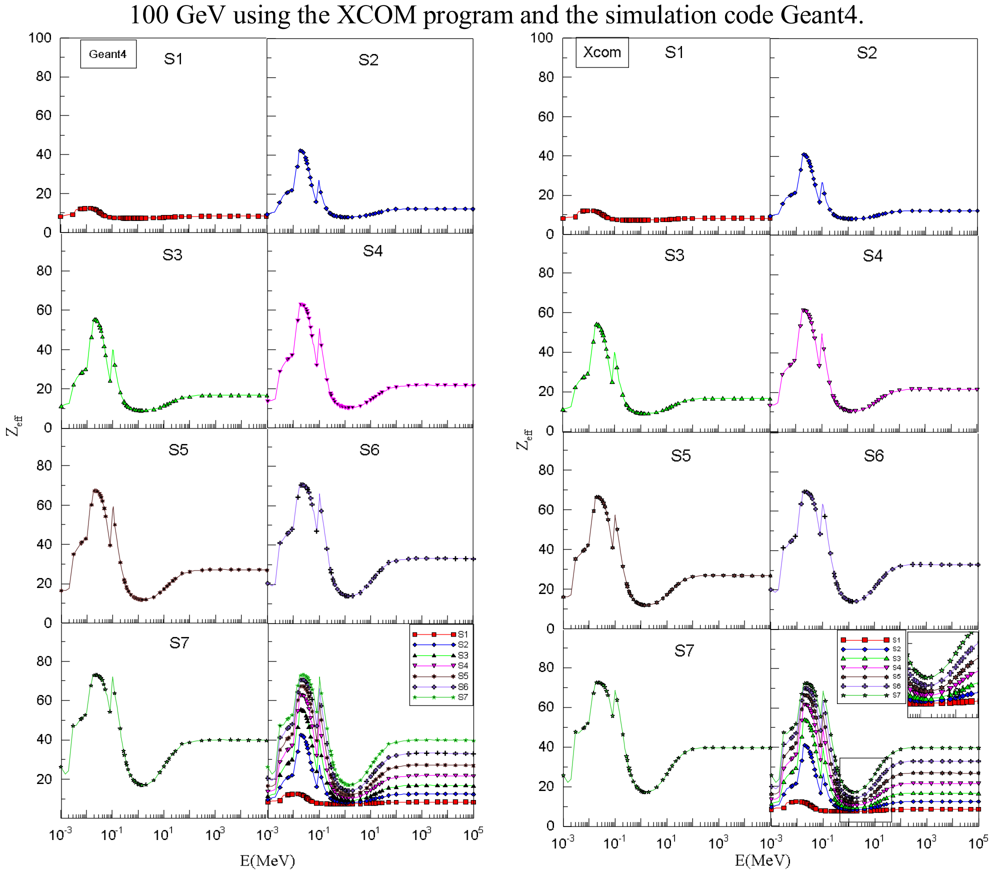

FIG. 9. Calculated effective atomic numbers (Z_{eff}) for the prepared samples against energy ranging from 1 keV to 100 GeV using the XCOM program and the simulation code Geant4.

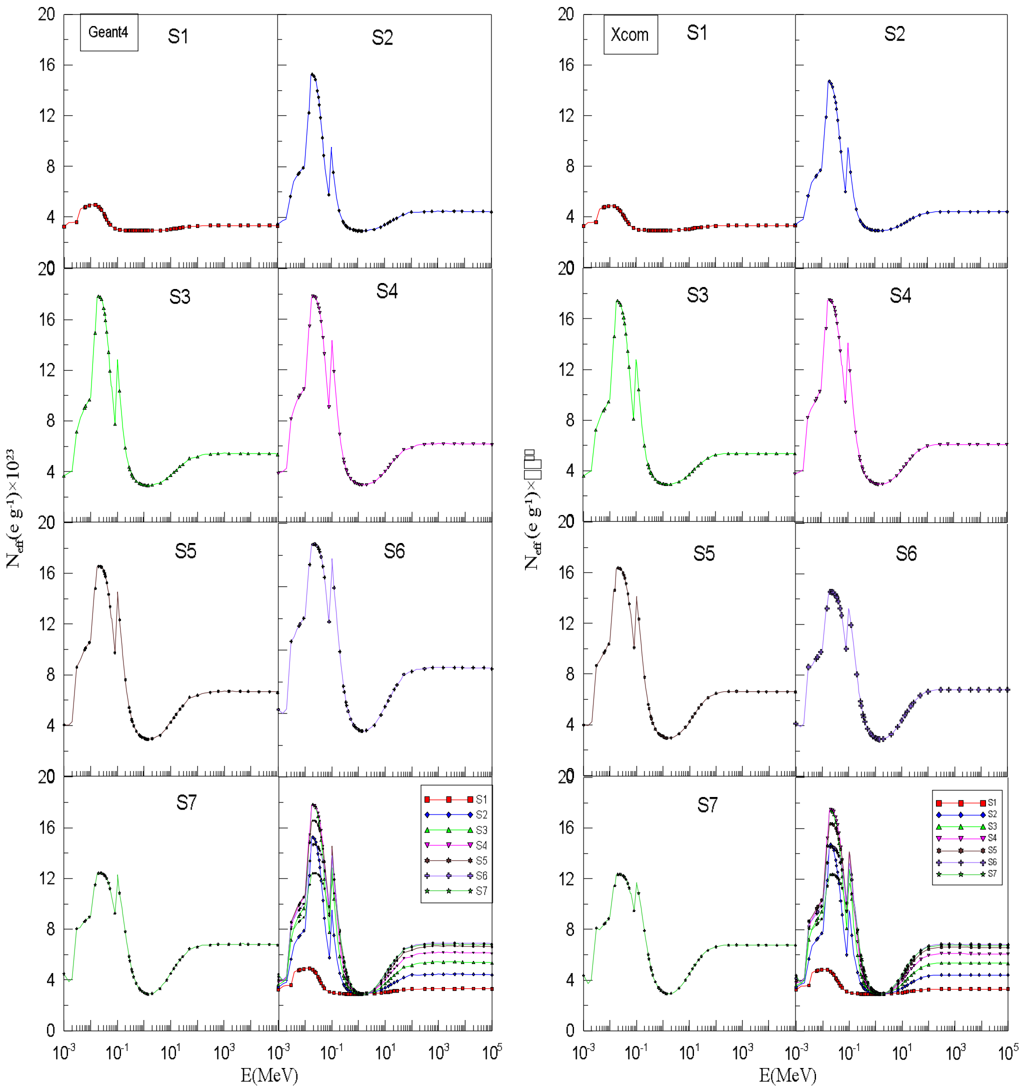

FIG. 10. Calculated effective electron numbers (N_{eff}) for the prepared samples against energy ranging from 1 keV to 100 GeV using the XCOM program and the simulation code Geant4.

Conclusions

The shielding parameters (μ_m, HVL, MFP, RPE, σ_a, σ_e, Z_{eff} and N_{eff}) of the investigated glass samples containing Li_2O, K_2O, Na_2O, PbO, and B_2O_3 have been calculated from 1 keV to 100 GeV as photon energy using the XCOM program and the simulation Monte Carlo code Geant4. The calculated results were compared with each other and with the experimental values at experimental data of 356.5, 662, 1173 and 1332 keV using a shielded Na(Tl) detector. Good agreement was obtained. It was found that the attenuation properties increased with the increase in the PbO concentration. The highest value of radiation protection efficiency was for sample S7 ($10Li_2O.10K_2O.20Na_2O.60PbO.0B_2O_3$), which has been found to be the most effective shielding material. The Z_{eff} and the N_{eff} values show a broad peak and a maximum value at 0.01 MeV and a minimum at 1 MeV. Above 1 MeV, the values tend to be constant. The used theoretical methods succeeded in describing the samples. Therefore, it will be preferable to obtain the photon shielding characteristics of the glass, particularly in cases where no experimental data exist. However, the XCOM program results were slightly higher than those given by the Geant4 code. Experimental data was lower than the theoretical values, where the Geant4 values are closer to the experiment.

References

[1] Ahmed, K.O., "Introduction to Health Physics", (Bookshop for Printing and Publishing, University of Mosul, 1993).

[2] Kaur, U., Sharma, J.K., Singh, P.S. and Singh, T., Applied Radiation and Isotopes, 70 (1) (2012) 233.

[3] Singh, C., Singh, T., Kumar, A. and Mudahar, G.S., Annals of Nuclear Energy, 31 (10) (2004) 1199.

[4] Bashter, I., Annals of Nuclear Energy, 24 (17) (1997) 1389.

[5] Wood, J., "Computational methods in reactor shielding", (Elsevier, Amsterdam, Netherlands, 2013).

[6] Krocher, J.F. and Browman, R.E., "Effects of Radiation on Materials and Components", Eds. Reinhold, (New York, 1984).

[7] Hubbell, J.H., International Journal of Applied Radiation and Isotopes, 33 (1982) 1269.

[8] Singh, K., Singh, H., Sharma, V., Nathuram, R., Khanna, A., Kumar, R. et al., Nuclear Instruments and Methods in Physics Research-Section B: Beam Interactions with Materials and Atoms, 194 (1) (2002) 1.

[9] Singh, K.J., Singh, N., Kaundal, R.S. and Singh, K., Nuclear Instruments and Methods in Physics Research B, 266 (2008) 944.

[10] Kirdsiri, K., Kaewkhao, J., Pokaipisit, A., Chewpraditkul, W. and Limsuwan, P., Annals of Nuclear Energy, 36 (2009) 1360.

[11] Kaewkhao, J. and Limsuwan, P., Nuclear Instruments and Methods in Physics Research A, 619 (2010) 295.

[12] Chanthima, N., Kaewkhao, J. and Limsuwan, P., Annals of Nuclear Energy, 41 (2012) 119.

[13] El-Kameesy, S.Y., Abd El-Ghany, S., Azooz, M.A. and El-Gammam, Y.A., World Journal of Condensed Matter Physics, 3 (2013) 198.

[14] El-Khayatt, A.M., Ali, A.M. and Singh, V.P., Nuclear Instruments and Methods in Physics Research A, 735 (2014) 207.

[15] Kaur, P., Singh, D. and Singh, T., Nuclear Engineering and Design, 307 (2016) 364.

[16] Kumar, A., Radiation Physics and Chemistry, 136 (2017) 50.

[17] El-Mallawany, R., Sayyed, M.I., Dong, M.G. and Rammah, Y.S., Radiation Physics and Chemistry, 151 (2018) 239.

[18] Shams, A.M.I., Tekin, H.O., Erguzel, T.T. and Susoy, G., Applied Physics A: Material Science and Processing, 125 (2019) 640.

[19] Shams, A.M.I., Yasser, B. Saddeek, M.I.S., Tekin, H.O. and Kilicoglu, O., Composites-Part B, 167 (2019) 231.

[20] Davisson, C.M., "Gamma-ray Attenuation Coefficients". In: Siegbahn (Ed.), Alpha-, beta- and gamma-ray spectroscopy (Vol. 1). (North Holland, Amsterdam, 1965).

[21] Taqi, A.H., Al Nuaimy, Q.A.M. and Gulalla, A.K., Journal of Radiation Research and Applied Sciences, 9 (2016) 256.

[22] Manohara, S.R. and Hanagodimath, S.M., Nucl. Instrum. Methods Phys. Res. B, 258 (2007) 321.

[23] Manohara, S.R., Hanagodimath, S.M., Thind, K.S. and Gerward, L., Nucl. Instrum. Methods Phys. Res. B, 266 (2008) 388.

[24] Taqi, A.H. and Khalil, H.J., Journal of Radiation Research and Applied Sciences, 10 (2017) 252.

[25] Rammah, Y.S., Abouhaswa, A.S., Salama, A.H. and El-Mallawany, R., Journal of Theoretical and Applied Physics, 13 (2019) 155.